RESEARCH ARTICLE

Au nanoparticles/g-C$_3$N$_4$ modified electrochemical biosensor for detection of gastric cancer miRNA based on hairpin locked nucleic acids probe

Mohammad Reza Mohammad Shafiee[1], Janan Parhizkar[2]*

[1] *Department of chemistry Faculty of Sciences, Islamic Azad University – Najafabad Branch, Najafabad, Iran.*

[2] *Nanotechnology Laboratory, Department of Chemistry, University of Isfahan, Isfahan, Iran.*

ARTICLE INFO

ABSTRACT

Objective(s): The annual incidence of cancer in the world is growing rapidly. The most important factor in the cure of cancers is their early diagnosis. miRNA, as a biomarker for detection of cancer in early stage, has attracted a lot of attention.

Methods: In this research, an electrochemical biosensor was designed to detect the amount of miR-106a, the biomarker of gastric cancer, by modifying a glassy carbon electrode (GCE) with a composite of g-C$_3$N$_4$ and Au nanoparticles. Complementary DNA strand of miR-106a which modified with biotin was used as a probe. Nanoparticles of titanium phosphate modified with Streptavidin and zinc ions were used to generate the electrochemical signal in square wave voltammetry. To identify the g-C$_3$N$_4$ functional group, the chemical composition of the titanium phosphate nanoparticles, the morphology and elemental composition of composite Fourier transform Infrared Spectroscopy, X-Ray Diffraction, Field Emission Scanning Electron Microscopy, and Energy Dispersive X-Ray Spectroscopy were used, respectively.

Results: The peaks of C, N, and Au in EDS spectrum confirmed composite formation. The linear range of the modified biosensor for miRNA-106a was obtained from 0.6 to 6.4 nM. The detection limit was calculated 80 pM.

Conclusions: Ultimately, Au nanoparticles/ g-C$_3$N$_4$ composite modified electrode can be a good platform for making electrochemical biosensor to diagnosis cancer in early stages.

INTRODUCTION

Gastric cancer is the fifth most common cancer and the third leading cause of cancer-related death worldwide. In most areas of the world, gastric cancer mortality has decreased markedly in recent decades. Nevertheless, gastric cancer stays a disease of poor prognosis and high mortality worldwide. Usually, the survival rate from gastric cancer is very low because the gastric cancer is diagnosed when the disease developed into a high pathological grade [1]. Gastric cancer is a multifunctional disease in which environmental and lifestyle factors are major reasons for getting gastric cancer [2, 3]. Usual strategies for the treatment of gastric cancer are not yet adequate. Perfect therapeutic targets should have two parameters: 1) causally associated with disease 2) suitable for designing therapeutic interventions while prophylaxis of gastric cancer can be more efficient and decline the cost imposed by this sickness. Prevention of gastric can be obtained at these levels:

i)   decreasing exposure to risk factors or by increasing the resistance to risk factors

ii)   Early detecting and treatment of disease. Screening has significant effect for individuals who are still in the preclinical phase

* Corresponding Author Email: *mohammad.r.mohammadshafiee@gmail.com*

iii) Treatment and rehabilitation and palliation to improve the outcome of illness in affected individuals [4].

Many efforts have been focused on early stage detection of gastric cancer. MicroRNAs (miRNAs) are small regions in RNAs of 20–22 nucleotides, which play an important role in all biological pathways in multicellular organisms [5].They are essential in the cell cycle, system balance and body health of human and can regulate gene expression level d [6,7]. Human health can be affected by miRNAs dysregulation more or less and directly and indirectly. Revealing the relationship between cancer and miRNAs has high importance and exigency for cancer diagnosis and curing. There are significantly different miRNA profiles between cancer cells and normal cells of the same tissue. According to scientific reports, some kinds of miRNAs are closely related to gastric cancer such as miRNAs-21[8, 9] and miR-106a [10]. The level of miR-106a in cancer tissues were notably higher than that in non-tumor tissues and appreciably related with tumor stage, size and differentiation; lymphatic and distant metastasis; and invasion [10]. Detection of miRNAs needs special techniques because of their small size, degradability, highly homologous sequences, and relatively low expression levels in cells [11, 12].

Electrochemical biosensors are one of the promising candidates to detect and determine miRNAs owing to their great advantages such as low cost, simplicity of construction and use, small size, high sensitivity and selectivity [13]. Electrochemical biosensors that utilize nanomaterials building units offer a lot of benefits such as enhancing the efficiency and sensitivity of the sensor [14]. Gold nanomaterials (Au nanoparticles, Au nanorods) and carbon nanomaterials (graphene oxide, CNT) are of the most known materials for modifying the electrodes surface [2, 15, 16, 17]. Using nanomaterials for the fabrication of biosensors increases the surface area for maximum detection. Cui et al have reported the fabrication of novel volatile biomarkers associated with gastric cancer cells and design a novel Au-Ag alloy composite-coated MWCNT for sensitive detection of volatile biomarkers[18].

Hairpin DNA probe, which was at first introduced in 1996, is a single-strand DNA molecule composed of a hairpin shaped oligonucleotide that possesses a stem and loop structure [19, 20]. DNA hairpins functionalized at one end with electroactive or fluorescent labels and immobilized onto substrates [21, 22]. The Hairpin-DNA probe has exhibited markedly stability, improved selectivity, and higher specificity than similar assays performed using linear single-strand DNA [23].

In this study, a sensitive hairpin DNA probe based on Zn^{2+} functionalized TiP nanospheres (TiP-Zn^{2+}) as a label was developed for the detection of gastric cancer biomarker (miR-106a). The Au nanoparticles/g-C_3N_4 composite modified GCE surface was applied to increase the selectivity and sensitivity of the sensor. The electrochemical signal was provided by Zn^{2+} ions which incorporated into the TiP nanospheres and bound to complementary strands by non-covalent interaction between biotin and Streptavidin.

EXPERIMENTAL

Materials and reagents

Biotin-terminated DNA probes and miR-106a sequences employed in this study (Table 1) were synthetic and purchased from Bioneer Corporation (South Korea). Milli-Q water (18MΩ cm resistivity) was used as a solvent for preparing of all solutions. Melamine ($C_3H_6N_6$), Mercaptopropionic acid ($C_3H_6O_4S$), chloroauric acid ($HAuCl_4$), poly (allylamine hydrochloride), bovine serum albumin, docusate sodium, and all other reagents were purchased from Sigma-Aldrich. For adjusting the pH of phosphate buffer saline (PBS), NaOH (0.1 M) and H_3PO_4 (0.1 M) aqueous solutions were used.

Apparatus

X-ray diffraction patterns recorded at room temperature, by BRUKER D8Advance X-ray diffractometer using CuKα radiation over the 2θ = 5-80°. The infrared spectrum was taken on FT-IR 6300 using KBr as the reference sample within a wavenumber range of 400 - 4000cm^{-1}.

Table 1. sequences of hairpin DNA probe and Target miRNA-106

name	sequences
hairpin DNA probe	5'-biotin-GGCCGCTACCTGCACTGTAAGCACTTTTCGGCC-(CH₂)₆SH-3'
Target miR-106a	5'-AAAAGUGCUUACAGUGCAGGUAG-3'

Energy dispersive X-ray spectroscopy (EDS) and Field emission scanning electron microscopy (FESEM) of the TESCAN (MIRA3) was used for investigating the elemental composition and morphology of composite, respectively. All electrochemical measurements were performed on a μAutolab III (Eco Chemie B.V.) potentiostat/galvanostat by NOVA 1.8 software. The utilized three-electrode system contained a platinum wire (auxiliary), a saturated calomel electrode (the reference), and the modified glassy carbon electrode with a diameter of 3 mm (working electrode). The potentials were reported with regards to the calomel electrode (reference).

Synthesis of Au nanoparticles/ g-C$_3$N$_4$ composite

For preparing bulk g-C$_3$N$_4$, melamine molecules were polymerized under heat treatment: first heating from 25°C till 600°C with ramp rate of about 5°C/min in air condition and then heating in 600°C for 2 hours. The color of the obtained product was yellow. To make g-C$_3$N$_4$ nanosheets, the bulk g-C$_3$N$_4$ was mill and 0.4 g of fine powder was dispersed in 800 ml and was exposed under ultrasonication. To remove the unexfoliated g-C$_3$N$_4$, obtained suspension was centrifuged at 5000 rpm and to obtain nanosheet, the upper dispersion of the previous stage was centrifuged at 15000 rpm. The nanosheets were dried in ambient condition.

6 mg of as-prepared g-C$_3$N$_4$ nanosheets was added in a 42 mL of HAuCl$_4$ (0.055 mM) aqueous solution. The mixture was stirred in the dark for 1 h, followed by adding 8 mL of methanol as a reducing agent and degassing under N$_2$ for 10 min. The mixture was stirred under visible light for 1 h in the ice water bath. Then, it was centrifuged at 15000 rpm [24]. A dispersion of Au/g-C$_3$N$_4$ composites in the water at a concentration of 1 mg mL^{-1} was prepared.

Preparation of Streptavidin–TiP– Zn^{2+} Ion Probes

Docusate sodium salt as the structure directing agent was dissolved into ethanol, and H$_3$PO$_4$ was added to get a turbid solution. A mixture of Tetrabutyl titanate with ethanol was dropped quickly into the Docusate sodium salt /ethanol solution. The mixture was put in a ultrasonic bath to obtain a stable mixture solution. The mixture was stirred at 70 °C for 7 h. To remove the residual phosphoric acid and surfactant, the solid product was washed with ethanol and deionized (DI) water for several times. To exchange ion, TiP nanospheres

were dispersed into 10 mM Zn(NO$_3$)$_2$ aqueous solution and stirred at 45 °C for 28 h. The hybrid nanospheres were separeted by centrifugation and rinsed with water several times. A dispersion of The TiP–Zn^{2+} in DI water with a concentration of 20 mg mL^{-1} was prepared. Next, the TiP–Zn^{2+} hybrids were dispersed into poly(allylamine hydrochloride) aqueous solution. After washing hybrids with DI water, the obtained hybrids dispersed into Glutaraldehyde (0.25 wt %), and sonicated. Hybrids were washed with DI and PBS three times and then, 600 μL of Streptavidin protein solution was added into the TiP–Zn^{2+} hybrids and shaken for 7 h. After centrifugation, the obtained bioconjugates were washed with PBS three times and resuspended in of tris buffer (pH = 7.4) [14].

Sensor fabrication

For modifying the surface of glassy carbon electrode (GCE) and preparing fresh surface, the GCE with a diameter of 3 mm was polished using alumina slurry followed by washing with water. Then GCE was sonicated in 1:1 nitric acid, acetone and water several times. The GCE was dried with N$_2$ flow. 10 μL of Au/g-C$_3$N$_4$ composite dispersion was dropped on the fresh GCE and dried at room temperature to obtained Au/g-C$_3$N$_4$ /GCE.

RNA Hybridization

The Locked Nucleic Acid incorporated DNA probe for avoiding the formation of dipolymer, was treated with a 70 °C water bath for 30min and then an ice-cold water bath for 10 min before immobilization. To immobilize the hairpin probe, the Au/g-C$_3$N$_4$/GCE was immersed in the immobilization buffer solution containing 1.0×10^{-7}M probe and 5.0×10^{-7}M Mercaptopropionic acid for 22 h. To remove the un-specifically immobilized probe and Mercaptopropionic acid, the modified electrode was rinsed three times with 10 mM Tris-HCl. For hybridization of the probe with miR-106a, the electrode was immersed into the hybridization buffer containing a known concentration of miR-106a for 1 h at 25°C in a humidified chamber. After this stage, the electrode was rinsed three times with the washing buffer to remove the un-hybridized miR-106a [25].

To bind the hybridized probe with signal tags, modified GCE was incubated with 10 μL of TiP–Zn^{2+}– Streptavidin bioconjugate solution for 60 min at 37 °C. To remove nonspecifically bound conjugates, it was washed with TBS [14].
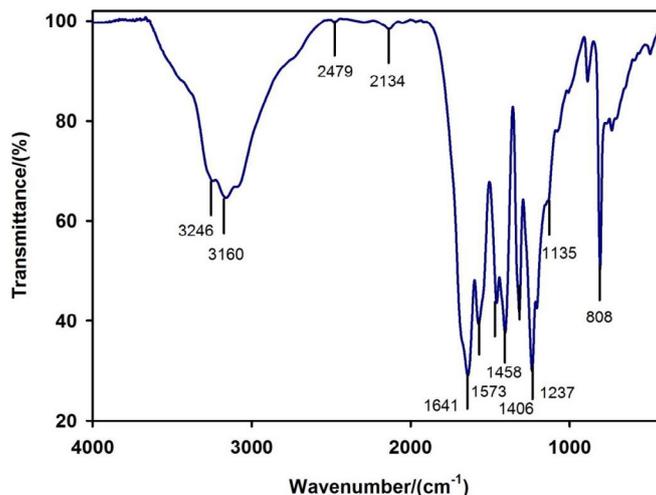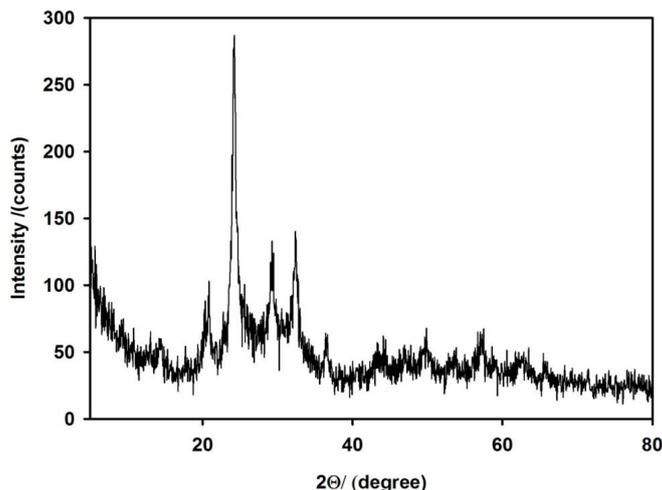
Fig.1. FTIR spectrum of g-C₃N₄

Fig.2. XRD pattern of TiP

Electrochemical Measurement

Square Wave Voltammetry (SWV) was used as the electrochemical method in 3 mL of HAc/NaAc buffer (pH =4.5, 0.2 mol L^{-1}). SWV scanning was done from −1.4 to −0.8 V with 25 mV pulse amplitude, 15 Hz pulse frequency, and 2 s quiet time. At about −1.1 V, the electrochemical responses were recorded for the measurement of miRNA.

RESULTS AND DISCUSSION
Characterization of g-C₃N₄

The chemical functional group of g-C₃N₄ surface was investigated by FTIR spectrum recorded between 4000-400 cm^{-1} (Fig.1).the peaks in the region from 700 to 1700 cm^{-1} are related to sp^2 C=N

stretching modes and out of plane bending vibration of sp^3 C-N bonds. The absorption peak observed at 808 cm^{-1}was associated with characteristic breathing mode of tri-s triazine cycles [26, 27]. The broad absorption peak at 3100-3300 cm^{-1} can be atributted to the stretching modes of secondary and primary amines and their intermolecular hydrogen bonding interactions [28].

Characterization of TiP

The crystal structure of TiP was determined by XRD (Fig.2). The diffraction peaks of TiP matched with its rhombohedral phase (JCPDS card 39-0004) and chemical formula (Ti₄P₆O₂₃). The reflection from the XRD pattern depicts the characteristic
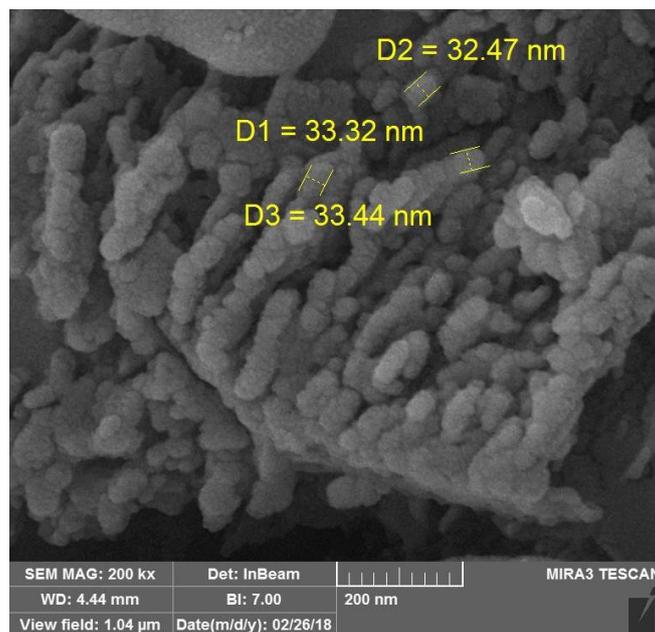
Fig.3. FESEM of Au nanoparticles /g-C$_3$N$_4$ nanocomposite

peaks (104), (113), (024), (116) and (030). The average crystallite size of Ti$_4$P$_6$O$_{23}$ was calculated using Scherrer`s equation (eq.1) and was found at about 41.22 nm.

$$D = \frac{0.9\lambda}{\beta \cos\theta} \qquad (1)$$

Where D is crystallite size, λ is the wavelength of Co kα radiation, β is the full width of half maximum of main intensity peak and θ is the brag`s angle.

Characterization of Au nanoparticles/ g-C$_3$N$_4$ nanocomposite

Field emission scanning electron microscope (FESEM) was employed to investigate the morphology of Au nanoparticles/ g-C$_3$N$_4$ nanocomposite (Fig.3). The sample for this analysis was obtained by evaporating water from Au/g-C$_3$N$_4$ composite dispersion in ambient condition. The FESEM figure from powder confirms the nanoscale dimension of the composite. The elemental composition of the composite was analyzed with EDS. Fig.4 shows EDS pattern of Au nanoparticles/ g-C$_3$N$_4$ nanocomposite. The peaks of C, N, and Au were observed in EDS spectrum.

Transduction pathway

This electrochemical biosensor consists of a modified working electrode with DNA probes.

Thiol terminated hairpin probes were connected to Au nanoparticles on the surface of electrode. When hairpin probes are closed biotins are trapped in probe structure and can`t bind to streptavidin. In presence of miR-106a (target miRNA) the hairpin DNA probes are opened and hybridization takes place with this ring opening, biotin obtains liberty and can interact with streptavidin on the surface of TiP-Zn^{2+} hybrids. The complementary hybrid of target miRNA and probe DNA act as electron wire. The Mercaptopropionic acid molecules block nonspecific sites on the surface of modified electrode. The electrochemical current responses of Zn^{2+} are used to measure the concentration of target miRNA. Fig.5 depicts the schematic of the modified electrode with hairpin probes and its performance. To obtain calibration curve different concentrations of target miRNA (6.4, 5, 4, 3, 1.8, 1.2, 1, 0.8, 0.6 nM) were applied and the electrochemical signals using SWV was measured.

The results showed that the increase of biosensor current was linearly related to the miR-106a concentration in the range from 0.6 nM to 6.4 nM. The regression equation was *I= 3.91 C-0.02* with a regression coefficient of 0.99. The detection limit was 80 pM (*DOL=3S$_0$*). Fig.6 depicts the calibration curve of Au nanoparticles/g-C$_3$N$_4$ modified GCE electrode in different concentration of miRNA-106A.
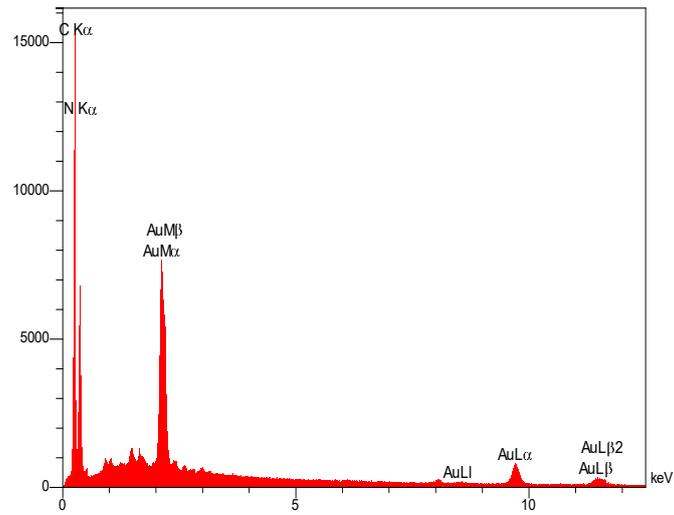
Fig.4. EDS spectrum of Au nanoparticles /g-C$_3$N$_4$ nanocomposite
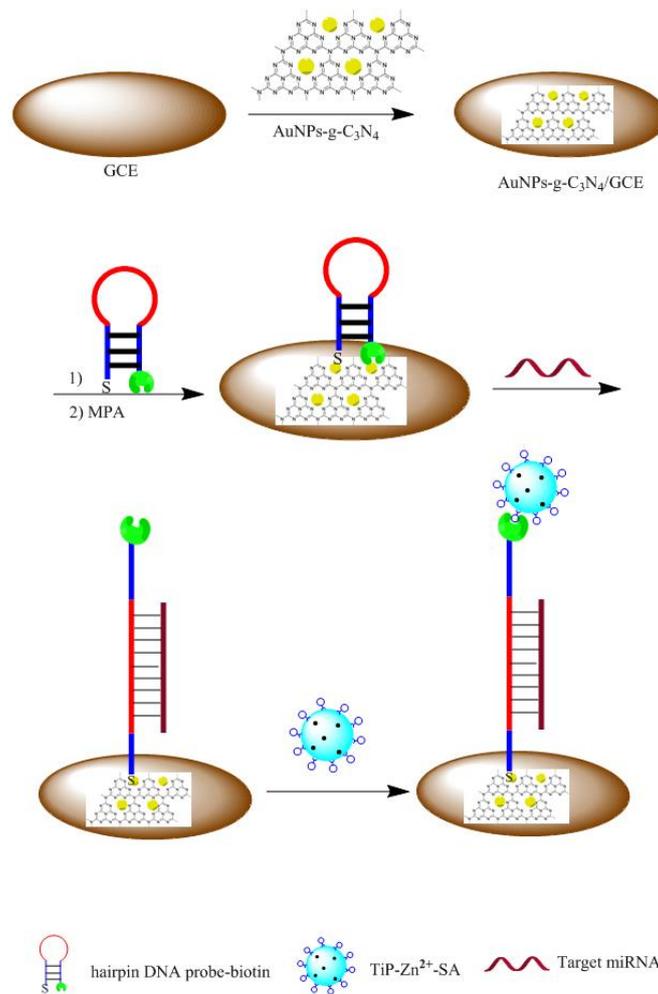

Fig.5. schematic illustration of Au nanoparticles/g-C$_3$N$_4$ composite modified electrode using hairpin DNA probe
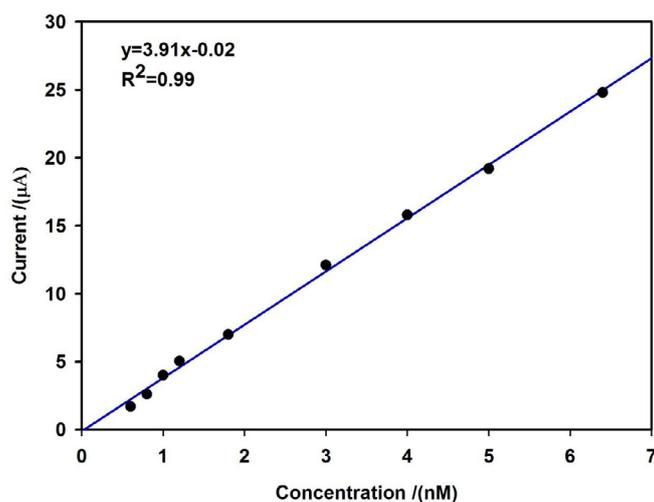
157

Fig.6. calibration curve of Au nanoparticles/g-C_3N_4 modified GCE electrode in different concentration of miRNA-106A

The precision of the sensor was evaluated by the assays of samples for five replicate measurements. The RSDs% (relative standard deviations) were 3.7, 2.2 and 1.8 for 10, 20, and 30nM miR-106a, respectively.

CONCLUSION

In summary, we have successfully fabricated a gastric cancer biosensor using hairpin DNA probe and Zn^{2+} functionalized TiP nanospheres labels. The hairpin electrochemical biosensor presents relatively sensitive miR-106a detection. There is a linear relationship between the SWV peak currents and the concentration of miR-106a in a range from o.6 nM to 6.4 nM with a detection limit to 80 pM.

CONFLICT OF INTERESTS

No conflict of interests was not reported by the authors.

REFERENCES

1. Thrift AP, El-Serag HB. Burden of Gastric Cancer. Clinical Gastroenterology and Hepatology. 2020;18(3):534-42.
2. Crew KD, Neugut AI. Epidemiology of gastric cancer. World Journal of Gastroenterology. 2006;12(3):354.
3. Zhang Y, Gao G, Liu H, Fu H, Fan J, Wang K, et al. Identification of Volatile Biomarkers of Gastric Cancer Cells and Ultrasensitive Electrochemical Detection based on Sensing Interface of Au-Ag Alloy coated MWCNTs. Theranostics. 2014;4(2):154-62.
4. Fock KM. Review article: the epidemiology and prevention of gastric cancer. Alimentary Pharmacology & Therapeutics. 2014;40(3):250-60.
5. Gurtan AM, Sharp PA. The Role of miRNAs in Regulating Gene Expression Networks. Journal of Molecular Biology. 2013;425(19):3582-600.
6. Song B, Ju J. Impact of miRNAs in gastrointestinal cancer diagnosis and prognosis. Expert Reviews in Molecular Medicine. 2010;12.
7. Chan SH, Wu CW, Li AFY, Chi CW, Lin WC. miR-21 microRNA expression in human gastric carcinomas and its clinical association. Anticancer research. 2008; 28(2A): 907-911.
8. Zhang Z, Li Z, Gao C, Chen P, Chen J, Liu W, et al. miR-21 plays a pivotal role in gastric cancer pathogenesis and progression. Laboratory Investigation. 2008;88(12):1358-66.
9. Simonian M, Mosallayi M, Mirzaei H. Circulating miR-21 as novel biomarker in gastric cancer: diagnostic and prognostic biomarker. Journal of cancer research and therapeutics. 2018; 14(2).
10. Hou X, Zhang M, Qiao H. Diagnostic significance of miR-106a in gastric cancer. International journal of clinical and experimental pathology. 2015; *8*(10): 13096.
11. Leshkowitz D, Horn-Saban S, Parmet Y, Feldmesser E. Differences in microRNA detection levels are technology and sequence dependent. RNA. 2013;19(4):527-38.
12. Lei J, Ju H. Signal amplification using functional nanomaterials for biosensing. Chemical Society Reviews. 2012;41(6):2122.
13. Niri A, Faridi-Majidi R, Saber R, Khosravani M, Adabi M. Electrospun carbon nanofiber-based electrochemical biosensor for the detection of hepatitis B virus. Biointerface Research in Applied Chemistry. 2019; 9(4);4022-4026.
14. Cheng F-F, He T-T, Miao H-T, Shi J-J, Jiang L-P, Zhu J-J. Electron Transfer Mediated Electrochemical Biosensor for MicroRNAs Detection Based on Metal Ion Functionalized Titanium Phosphate Nanospheres at Attomole Level. ACS Applied Materials & Interfaces. 2015;7(4):2979-85.
15. Loo F-C, Ng S-P, Wu C-ML, Kong SK. An aptasensor using DNA aptamer and white light common-path SPR spectral interferometry to detect cytochrome-c for anti-cancer drug screening. Sensors and Actuators B: Chemical. 2014;198:416-23.
16. Huang H, Bai W, Dong C, Guo R, Liu Z. An ultrasensitive electrochemical DNA biosensor based on graphene/Au

nanorod/polythionine for human papillomavirus DNA detection. Biosensors and Bioelectronics. 2015;68:442-6.

17. Cheng N, Tian J, Liu Q, Ge C, Qusti AH, Asiri AM, et al. Au-Nanoparticle-Loaded Graphitic Carbon Nitride Nanosheets: Green Photocatalytic Synthesis and Application toward the Degradation of Organic Pollutants. ACS Applied Materials & Interfaces. 2013;5(15):6815-9.

18. Gulati P, Kaur P, Rajam MV, Srivastava T, Mishra P, Islam SS. Single-wall carbon nanotube based electrochemical immunoassay for leukemia detection. Analytical Biochemistry. 2018;557:111-9.

19. Riccelli PV. Hybridization of single-stranded DNA targets to immobilized complementary DNA probes: comparison of hairpin versus linear capture probes. Nucleic Acids Research. 2001;29(4):996-1004.

20. Abolhasan R, Mehdizadeh A, Rashidi MR, Aghebati-Maleki L, Yousefi M. Application of hairpin DNA-based biosensors with various signal amplification strategies in clinical diagnosis. Biosensors and Bioelectronics. 2019;129:164-74.

21. Zhang D, Gao Q, Peng Y, Qi H, Zhang C. Label-free electrochemical DNA biosensor array for simultaneous detection of the HIV-1 and HIV-2 oligonucleotides incorporating different hairpin-DNA probes and redox indicator Electrolysis of coal slurries to produce hydrogen gas Biosensors and Bioelectronics. 2010, 25(5): 1088-1094.

22. Li Z, Huang P, He R, Lin J, Yang S, Zhang X, et al. Aptamer-conjugated dendrimer-modified quantum dots for cancer cell targeting and imaging. Materials Letters. 2010;64(3):375-8.

23. Zhang J, Qi H, Li Y, Yang J, Gao Q, Zhang C. Electrogenerated Chemiluminescence DNA Biosensor Based on Hairpin DNA Probe Labeled with Ruthenium Complex. Analytical Chemistry. 2008;80(8):2888-94.

24. Wang S, Li D, Sun C, Yang S, Guan Y, He H. Synthesis and characterization of g-C3N4/Ag3VO4 composites with significantly enhanced visible-light photocatalytic activity for triphenylmethane dye degradation. Applied Catalysis B: Environmental. 2014;144:885-92.

25. Zhou Y, Zhang Z, Xu Z, Yin H, Ai S. MicroRNA-21 detection based on molecular switching by amperometry. New Journal of Chemistry. 2012;36(10):1985.

26. Wen J, Xie J, Chen X, Li X. A review on g-C 3 N 4 -based photocatalysts. Applied Surface Science. 2017;391:72-123.

27. Zhu J, Xiao P, Li H, Carabineiro SAC. Graphitic Carbon Nitride: Synthesis, Properties, and Applications in Catalysis. ACS Applied Materials & Interfaces. 2014;6(19):16449-65.

28. Lotsch BV, Schnick W. From Triazines to Heptazines: Novel Nonmetal Tricyanomelaminates as Precursors for Graphitic Carbon Nitride Materials. Chemistry of Materials. 2006;18(7):1891-900.